Cascade luminescent solar concentrators

Sthy Flores Daorta,[1] Antonio Proto,[2] Roberto Fusco,[2] Lucio Claudio Andreani,[1] and Marco Liscidini[1]
[1]*Dipartimento di Fisica, Università degli Studi di Pavia, Via Bassi 6, 27100 Pavia, Italy*
[2]*ENI S.p.A, Research Center for Non-Conventional Energies—Istituto ENI Donegani, Via Fauser 4, 28100 Novara, Italy*

(Received 13 March 2014; accepted 3 April 2014; published online 14 April 2014)

We propose a luminescent solar concentrator (LSC) characterized by a strong enhancement of the concentration factor in which the area covered by photovoltaic cells is independent of the area over which sunlight is collected. We name this device cascade-LSC (c-LSC), as sunlight is both geometrically and spectrally concentrated by cascading absorption and emission into different LSCs. We demonstrate a prototype and measure the generated photocurrent. The results are in good agreement with those predicted by our numerical model based on Monte Carlo simulations. © *2014 AIP Publishing LLC*. [http://dx.doi.org/10.1063/1.4871481]

In the last few years, we have seen a bourgeoning interest in photovoltaic (PV) research with the goal of reducing the cost of solar energy. To this end, most of the efforts have been focused on decreasing the cost of PV cells while maintaining or improving their efficiency. An alternative strategy is based on light concentrators, which are able to collect sunlight over large areas and redirect it onto small and efficient PV devices, thus reducing the impact of PV cells on the total cost of energy production. The most common and utilized concentrators are composed of mirrors and lenses that redirect and focus sunlight exploiting geometrical optics. This solution has good performances, but it requires sun track-systems, which inevitably imply costs of installation and maintenance.

A second approach to sunlight concentration makes use of dielectric slabs doped with fluorescent dyes (see Fig. 1(a)). In these structures, known as luminescent solar concentrators (LSCs), sunlight is absorbed by the dyes and subsequently remitted at lower energies. Most of the re-emitted light is guided in the slab by total internal reflection (TIR) and then converted to photocurrent by the PV cells attached to the lateral slab edges. Since the typical efficiency of LSCs is only a few percent, they are not yet able to compete with traditional concentrators for cost effective energy production. Still, the flexibility of LSCs in terms of materials and shapes stimulates new research and suggests various applications, for example, as semi-transparent elements in modern architecture.[1]

The first reference on LSCs for solar applications appeared in the 70s.[2,3] Since then, the form of LSCs has not changed substantially. The performances of LSCs are directly related to the absorption and emission spectra of the embedded dyes, which set the fraction of sunlight that can be absorbed and determine the propagation losses in the slab due to self-absorption of the emitted light. Thus, most of the research has been focused on the use of different emitters, including organic dyes,[1,4–6] quantum dots,[7–10] and rare earths.[11–13] Other strategies to reduce self-absorption and increase the efficiency of LSCs are based on the optimization of their structure, for example, by means of scatterers[14–16] and plasmonics nanoparticles,[17,18] inhomogenous distribution of the dyes,[19–21] and realization of LSCs with different shapes.[14,22–25]

In this work, we introduce the concept of cascade LSC (c-LSC). The device is shown in Fig. 1(b), and it is composed of a large LSC, named the primary, surrounded by four smaller LSCs, named secondaries, having PV cells attached on their smallest facets. The working principle is based on the combination of two different kinds of LSCs: the primary-LSC contains dyes that are able to absorb in the desired spectral region of the incident sunlight, the secondary-LSCs contain dyes whose absorption spectrum is matched to the emission bandwidth of the primary-LSC. Thus, by cascading the LSCs one increases both the spectral and the geometrical concentration of light, along with a strong reduction of the area covered by PV cells. Indeed, unlike traditional concentrators (see Fig. 1(a)), in a c-LSC the area covered by PV cells is independent of the area over which sunlight is collected.

The choice of the optimal dye in each element of the c-LSC depends mainly on two factors: the fraction of sunlight spectrum (see Fig. 2(a)) that one wants to absorb, which may

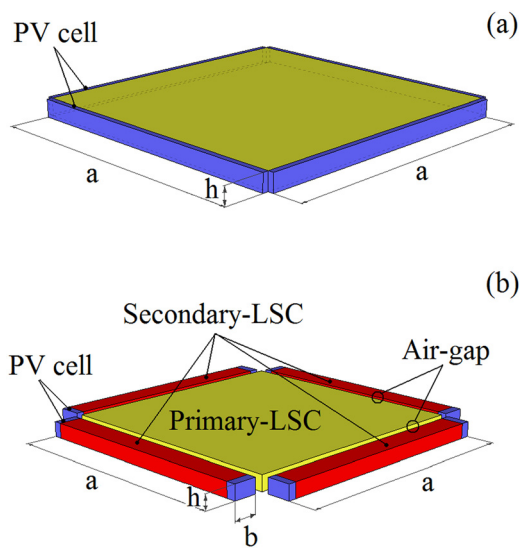

FIG. 1. Sketch of a traditional LSC (a) and a c-LSC (b).

 © 2014 AIP Publishing LLC

This article is copyrighted as indicated in the article. Reuse of AIP content is subject to the terms at: http://scitation.aip.org/termsconditions. Downloaded to IP: 151.65.244.70 On: Sun, 11 May 2014 09:17:21

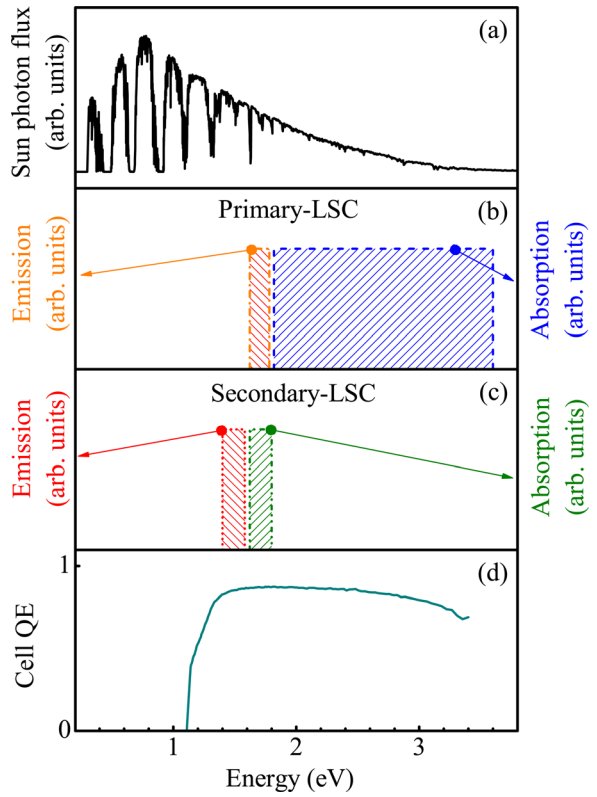

FIG. 2. Sun photon flux (a), ideal absorption and emission spectra of the dye in the primary (b), ideal absorption and emission spectra of the dye in the secondary-LSC (c), and quantum efficiency of the Si-PV cell (d) as a function of the photon energy.

vary depending on the final application of the LSC (e.g., a semi-transparent windows in a greenhouse or an opaque element to generate electric energy) and the spectral quantum efficiency of the PV cells (e.g., see Fig. 2(d)). Idealized absorption and emission spectra of the dyes that could be utilized in the primary- and secondary-LSCs are shown in Figs. 2(b) and 2(c), respectively. In particular, one looks for dyes with a small or negligible superposition between absorption and emission spectra to inhibit re-absorption losses, which are one of the main factors that limit light concentration. Unfortunately, dyes characterized by a large Stokes' shift of absorption and emission spectra have usually a limited absorption bandwidth, and viceversa. Thus, in conventional LSCs or in the primary concentrator of a c-LSC, one has to reach a compromise between absorption bandwidth and Stokes shift. This is not the case for the secondary-LSC for which the absorption bandwidth can be pretty narrow, as it is targeted to the emission spectrum of the primary-LSC rather than sunlight. This makes it possible to choose dyes characterized by a much larger Stokes shift and to improve the light propagation length.

Even if one can find dyes with negligible superposition of absorption and emission spectra, the efficiency of a LSC is intrinsically limited by the fraction of emitted light that can be guided by TIR. For the LSC shown in Fig. 1(a), which has the shape of a rectangular slab, this depends only on the refractive indices of the slab (typically made of plastic or glass, $n_{slab} \cong 1.5$) and of the surrounding medium (typically air, $n_{clad} \cong 1$). The probability that a photon absorbed in the slab reaches the PV cells on the lateral facets is $p_{LSC} = 0.74$, and it can be calculated as $p_{LSC} = 1 - 2f$, where $f = 0.13$ is the fraction of light emitted by the dye above the critical angle for total internal reflection at n_{slab}/n_{clad} interface.

The previous calculation can also be done for the c-LSC shown in Fig. 1(b). In this case, one has to consider that the light concentrated by the primary-LSC on its lateral facets is then absorbed and re-emitted in the secondary-LSC. For the geometry presented in Fig. 2(b), light is collected only on two facets of each secondary-LSC; thus, the collection probability for the c-LSC is $p_{c\text{-}LSC} = (1 - 2f)(1 - 4f) = 0.355$.

If we assume that the LSC and the primary-LSC of Figs. 1(a) and 1(b) are identical and that the quantum efficiency of the PV cells is the same in the emission range of the dyes embedded in the primary- and secondary-LSCs, the ratio $p_{c\text{-}LSC}/p_{LSC}$ is exactly the ratio of the efficiencies of the two concentrators. On the one hand, this means that the ultimate efficiency of a c-LSC is only about half the efficiency of a traditional LSC. On the other hand, the amount of surface covered by PV cells in a c-LSC is smaller than in a traditional LSC, for example, less than 50 times if we consider typical dimensions $a = 100$ cm and $b = h = 1$ cm.

This analysis is based only on simple geometrical arguments, which are independent of choice of the dyes. Yet, an important limit to sunlight concentration is indeed set by the dye absorption spectrum, which is typically narrower than that of conventional PV cells. Thus, to evaluate the performances of a LSC, one has to calculate the photocurrent density generated by the LSC under sunlight illumination and compares it with the photocurrent density that would be obtained by direct illumination of the PV cells. This leads to the effective concentration factor

$$CF_{eff} = \frac{J_{concentrator}}{J_{PV\ cell}}, \tag{1}$$

which measures the real concentration capability of the device. We have effective concentration of sunlight when $CF_{eff} > 1$.

We want to calculate the CF_{eff} for the c-LSC shown in Fig. 1. We considered a PMMA slab doped with dithiophen-benzothiadiazole (DTB) with a concentration of 100 ppmm as primary-LSC and four PMMA slabs doped with Lumogen F-Red 305 (Fred305) with a concentration of 160 ppmm as secondary-LSCs. The absorption and emission spectra of the dyes are shown in the Figures 3(b) and 3(c), respectively. Finally, we consider eight Si-cells characterized by the quantum efficiency shown in Fig. 3(d) and a short circuit current density $J_{sc} = 34\,\mathrm{mA/cm^2}$. We calculated the photocurrent density generated by the c-LSC by means of a numerical method based on a Monte Carlo approach[26–28] that is able to describe the propagation losses induced by self-absorption. The CF_{eff} as a function of a, assuming $b = h = 0.6$ cm, is shown in Fig. 4 along with the effective concentration factor calculated for the LSC of Fig. 1(a), where we have considered a PMMA slab doped with DTB with a concentration of 100 ppmm. The results show that the c-LSC outperforms the LSC in terms of effective concentration factor, and that the CF_{eff} of a c-LSC can be larger than 4 for a side length $a = 80$ cm. This value depends mainly on the choice of the dye in the primary LSC, which determines the fraction of sunlight that is absorbed. As mentioned

This article is copyrighted as indicated in the article. Reuse of AIP content is subject to the terms at: http://scitation.aip.org/termsconditions. Downloaded to IP: 151.65.244.70 On: Sun, 11 May 2014 09:17:21

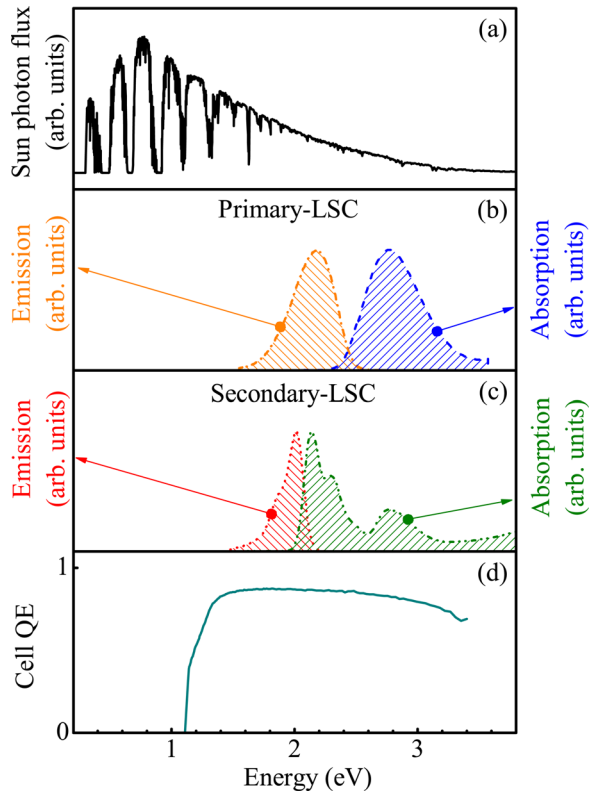

FIG. 3. Sun photon flux (a), absorption and emission spectra of the DTB (b), absorption and emission spectra of the FRed305 (c), and quantum efficiency of the Si-PV cell (d) as a function of the photon energy.

above, the dye optimization depends on the final use of the LSCs and is beyond the scope of this work. Yet, for the geometry considered here, it should be noticed that the maximum CF_{eff} is 0.355 (a^2/h^2), namely, the fraction of light trapped by TIR times the geometrical concentration factor.

To demonstrate the c-LSC, we built and characterized the prototype shown in Fig. 5. The primary-LSC is a 11 cm × 11 cm × 0.6 cm PMMA slab doped with DTB with a concentration of 100 ppmm. The secondary-LSCs are four identical 10.8 cm × 0.6 cm × 0.6 cm PMMA slabs doped with Lumogen F-Red 305 (Fred305) with a concentration of 160 ppmm (see Figs. 3(b) and 3(c)). Finally, the eight PV cells are Si-cells XOB17-12 × 1, manufactured by IXIS,

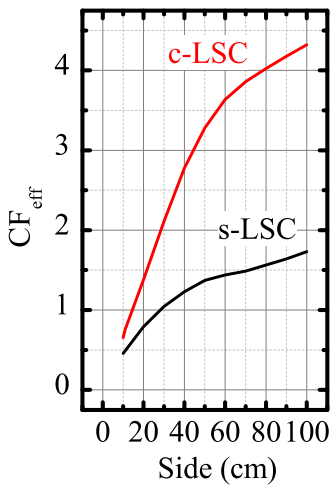

FIG. 4. Effective concentration factor for s-LSC and c-LSC.

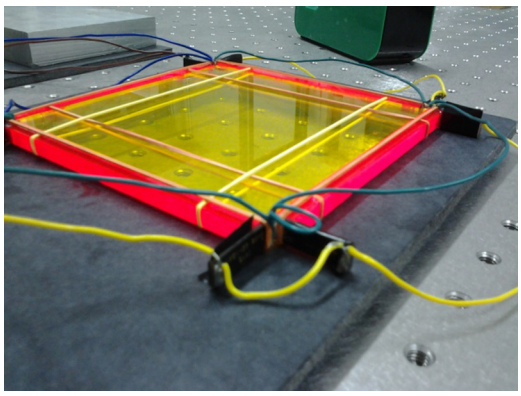

FIG. 5. Picture of the prototype in PMMA of the c-LSC assembled using a square slab doped with DTB, and four bars doped with Fred305.

having dimensions 22 mm × 7 mm × 1.6 mm, open circuit voltage $V_{oc} = 630$ mV, short circuit current density $J_{sc} = 34$ mA/cm^2, and efficiency $\eta = 17\%$ (see Fig. 3(d)). The PV cells are connected in parallel and, since they are larger than secondary-LSC facets, the part of each cell exceeding the facet is covered with a black tape.

The c-LSC was illuminated by a Sun 2000 Solar Simulator manufactured by Abet Technologies, which is able to reproduce the irradiance spectrum AM 1.5G according to the standard ASTM 927-05 on an area of 11 cm × 11 cm. We measured a photocurrent of 65 mA, which corresponds to $J_{sc,c\text{-}LSC} = 22.6$ mA/cm^2 and to $CF_{eff,c-LSC} = 0.67$. It should be noticed that for such a small prototype, whose dimensions are limited by the specifications of our solar simulator, a $CF_{eff} < 1$ is expected, and it is in good agreement with the theoretical results showed in Fig. 4. We repeated the same experiment with a traditional LSC made of the 11 cm × 11 cm × 0.6 cm PMMA slab doped with DTB (i.e., the primary-LSC) in the configuration of Fig. 1(a). In this case, we measured a current of 388 mA, which corresponds to $J_{sc,LSC} = 14.7$ mA/cm^2 and $CF_{eff,LSC} = 0.43$. Again, the result is in good agreement with those shown in Fig. 4, and it demonstrates that the c-LSC is able to concentrate 55.6% more than the corresponding traditional LSC.

It has to be mentioned that the experimental efficiency of our prototype is low in absolute terms. Yet, this is not an intrinsic limitation of the c-LSC itself, but it depends on both the concentrator dimensions and the spectral properties of the dyes used in our proof-of-concept. In particular, DTB and Lumogen F-Red 305 (Fred305), which have been developed with applications to conventional LSCs, have absorption and emission spectra very different from the ideal ones shown in Figs. 2(b) and 2(c). Clearly, c-LSCs require the use of specific dyes, especially for what concerns the secondary-LSCs.

In conclusion, we have proposed the concept of c-LSC in which the area covered by PV cells is independent of the area over which sunlight is collected. In this kind of concentrators, the combination of two different types of LSCs allows one to obtain an effective concentration factor that is larger than that achievable with traditional LSCs. We also built and characterized a prototype based on dyes typically implemented in LSCs. The results are well described by our

This article is copyrighted as indicated in the article. Reuse of AIP content is subject to the terms at: http://scitation.aip.org/termsconditions. Downloaded to IP: 151.65.244.70 On: Sun, 11 May 2014 09:17:21

theoretical model. Given the high concentration factor that characterized this device, we believe this approach might be attractive for a further development of LSCs as well as appealing in the field of optical detection.

This work was supported by ENI S.p.A. through research programme "Along with Petroleum—Materiali fotoattivi" under Contract No. 3500019461.

[1]M. G. Debije and P. P. C. Verbunt, Adv. Energy Mater. **2**, 12 (2012).
[2]W. H. Weber and J. Lambe, Appl. Opt. **15**, 2299 (1976).
[3]J. A. Levitt and W. H. Weber, Appl. Opt. **16**, 2684 (1977).
[4]R. O. Al-Kaysi, T. S. Ahn, A. M. Müller, and C. J. Bardeen, Phys. Chem. Chem. Phys. **8**, 3453 (2006).
[5]M. A. El-Shahawy and A. F. Mansour, J. Mater. Sci. Mater. Electron. **7**, 171 (1996).
[6]J. M. Drake, M. L. Lesiecki, J. Sansregret, and W. R. L. Thomas, Appl. Opt. **21**, 2945 (1982).
[7]S. M. Reda, Acta Mater. **56**, 259 (2008).
[8]A. J. Chatten, K. W. J. Barnham, B. F. Buxton, N. J. Ekins-Daukes, and M. A. Malik, Semiconductors **38**, 909 (2004).
[9]S. J. Gallagher, B. Norton, and P. C. Eames, Sol. Energy **81**, 813 (2007).
[10]S. J. Gallagher, P. C. Eames, and B. Norton, Int. J. Ambient Energy **25**, 47 (2004).
[11]J. C. Goldschmitd, "Novel solar cell concepts," Ph.D. thesis (Universität Konstanz, 2009).
[12]O. Moudam, B. C. Rowan, M. Alamiry, P. Richardson, B. S. Richards, A. C. Jones, and N. Robertson, Chem. Commun. **43**, 6649 (2009).
[13]L. J. Andrews, B. C. McCollum, and A. Lempicki, J. Lumin. **24–25**, 877 (1981).
[14]W. G. J. H. M. van Sark, K. W. J. Barnham, L. H. Slooff, A. J. Chatten, A. Büchtemann, A. Meyer, S. J. McCormack, R. Koole, D. J. Farrell, R. Bose, E. E. Bende, A. R. Burgers, T. Budel, J. Quilitz, M. Kennedy, T. Meyer, C. D. M. Donegá, A. Meijerink, and D. Vanmaekelbergh, Opt. Express **16**, 21773 (2008).
[15]A. Goetzberger, Appl. Phys. **16**, 399 (1978).
[16]R. Sóti, É. Farkas, M. Hilbert, Z. Farkas, and I. Ketskeméty, J. Lumin. **68**, 105 (1996).
[17]T. K. Sau, A. L. Rogach, F. Jäckel, T. A. Klar, and J. Feldmann, Adv. Mater. **22**, 1805 (2010).
[18]H. R. Wilson, Sol. Energy Mater. **16**, 223 (1987).
[19]M. J. Currie, J. K. Mapel, T. D. Heidel, S. Goffri, and M. A. Baldo, Science **321**, 226 (2008).
[20]A. Goetzberger and W. Greube, Appl. Phys. **14**, 123 (1977).
[21]S. Tsoi, D. J. Broer, C. W. Bastiaansen, and M. G. Debije, Opt. Express **18**, A536 (2010).
[22]M. Sidrach de Cardona, M. Carrascosa, F. Meseguer, F. Cusso, and F. Jaque, Sol. Cells **15**, 225 (1985).
[23]A. H. Zewail and J. S. Batchelder, U.S. patent 4,227,939 (14 October 1980).
[24]J. S. Batchelder, A. H. Zewail, and T. Cole, Appl. Opt. **20**, 3733 (1981).
[25]K. R. McIntosh, N. Yamada, and B. S. Richards, Appl. Phys. B **88**, 285 (2007).
[26]M. Carrascosa, S. Unamuno, and F. Agullo-Lopez, Appl. Opt. **22**, 3236 (1983).
[27]S. Flores, M. Liscidini, L. Andreani, P. Scudo, and R. Fusco, in *Proceeding of the 26th European Photovoltaic Solar Energy Conference and Exhibition* (Hamburg, Germany, 2011), pp. 264–267.
[28]R. Y. Rubinstein and D. P. Kroese, *Simulation and the Monte Carlo Method* (Wiley, 2008).

This article is copyrighted as indicated in the article. Reuse of AIP content is subject to the terms at: http://scitation.aip.org/termsconditions. Downloaded to IP: 151.65.244.70 On: Sun, 11 May 2014 09:17:21